Mutagenic potency of *Helicobacter pylori* in the gastric mucosa of mice is determined by sex and duration of infection

Alexander Sheh[a], Chung Wei Lee[a,b], Kenichi Masumura[c], Barry H. Rickman[b], Takehiko Nohmi[c], Gerald N. Wogan[a,1], James G. Fox[a,b,2], and David B. Schauer[a,b,2]

[a]Department of Biological Engineering, Massachusetts Institute of Technology, Cambridge, MA 02139; [b]Division of Comparative Medicine, Massachusetts Institute of Technology, Cambridge, MA 02139; and [c]Division of Genetics and Mutagenesis, National Institute of Health Sciences, Tokyo 158-8501, Japan

Contributed by Gerald N. Wogan, July 19, 2010 (sent for review April 27, 2010)

***Helicobacter pylori* is a human carcinogen, but the mechanisms evoked in carcinogenesis during this chronic inflammatory disease remain incompletely characterized. We determined whether chronic *H. pylori* infection induced mutations in the gastric mucosa of male and female *gpt* delta C57BL/6 mice infected for 6 or 12 mo. Point mutations were increased in females infected for 12 mo. The mutation frequency in this group was 1.6-fold higher than in uninfected mice of both sexes ($P < 0.05$). A:T-to-G:C transitions and G:C-to-T:A transversions were 3.8 and 2.0 times, respectively, more frequent in this group than in controls. Both mutations are consistent with DNA damage induced by oxidative stress. No increase in the frequency of deletions was observed. Females had more severe gastric lesions than males at 6 mo postinfection (MPI; $P < 0.05$), but this difference was absent at 12 MPI. In all mice, infection significantly increased expression of *IFNγ*, *IL-17*, *TNFα*, and *iNOS* at 6 and 12 mo, as well as *H. pylori*–specific IgG1 levels at 12 MPI ($P < 0.05$) and IgG2c levels at 6 and 12 MPI ($P < 0.01$ and $P < 0.001$). At 12 MPI, IgG2c levels in infected females were higher than at 6 MPI ($P < 0.05$) and also than those in infected males at 12 MPI ($P < 0.05$). Intensity of responses was mediated by sex and duration of infection. Lower *H. pylori* colonization indicated a more robust host response in females than in males. Earlier onset of severe gastric lesions and proinflammatory, Th1-biased responses in female C57BL/6 mice may have promoted mutagenesis by exposing the stomach to prolonged oxidative stress.**

gpt delta mouse | *Helicobacter* | inflammation | mutagenesis | sexual dimorphism

Acting through multiple, complex mechanisms that are incompletely understood, chronic inflammation is a significant risk factor for several major human malignancies, including stomach cancer. Chronic inflammation induced by *Helicobacter pylori* infection increases lifetime risk of developing gastritis, duodenal and gastric ulcers, mucosa-associated lymphoid tissue lymphoma, mucosal atrophy, and gastric carcinoma (1, 2). Indeed, *H. pylori* has been classified by International Agency for Research on Cancer as a group I human carcinogen on the basis of its impact on gastric cancer incidence, the second most frequent cause of cancer-related death worldwide (3). Among postulated mechanisms through which infection may contribute to increased cancer risk are overproduction of reactive oxygen and nitrogen species (RONS) by inflammatory cells, and the consequent induction of mutations critical for tumor initiation in cells of inflamed tissues (4). The inflammatory response to infection results in increased production of RONS, including superoxide ($O_2^{-}\cdot$), hydrogen peroxide (H_2O_2), nitric oxide (NO), peroxynitrite (ONO_2^{-}), and nitrous anhydride (N_2O_3), in vitro (5, 6) and in vivo (7–9). *H. pylori* can also directly activate RONS-producing enzymes, such as inducible NO synthase (iNOS) and spermine oxidase, in gastric epithelial cells, causing DNA damage and apoptosis (5, 6). Chronic inflammatory states increase levels of DNA adducts, such as etheno adducts, 8-oxoG, and other mutagenic precursors, in vitro and in vivo (10–12), but tend not to alter the frequency of deletions (13). RONS also can damage DNA indirectly by creating adduct-forming electrophiles via lipid peroxidation (14, 15). RONS have been shown to induce mutations in *H. pylori* by inducing a hypermutation state in the bacteria (16).

A widely used experimental model is the *H. pylori* SS1-infected C57BL/6 mouse, which is susceptible to chronic infection and develops robust gastritis and premalignant lesions similar to those occurring in humans (17, 18). To date, limited investigation has focused on genetic damage associated with infection in these animals, but available data are still incomplete. Enhanced DNA fragmentation was observed in gastric cells of infected mice (19), in which dsDNA breaks were also detected by TUNEL assay (20, 21). Mutagenicity in reporter genes recovered from gastric DNA of male and female Big Blue transgenic mice 6 mo after infection with *H. pylori* or *Helicobacter felis* has also been reported (22). In *H. pylori*-infected male mice, point mutation frequency was increased at 6 mo post infection (MPI), but decreased to control levels by 12 MPI, suggesting that the animals may have adapted to infection (22). Female mice infected with *H. felis* also had an increased frequency of point mutations at 7 MPI, compared with uninfected controls (23). Mutagenesis resulting from infection has also been associated with p53 status. Mutations were found in the *lacI* reporter genes of a small number of *H. felis*-infected female TSG-p53/Big Blue mice harboring either one ($p53^{+/-}$) or two ($p53^{+/+}$) WT p53 alleles (23). A 2-fold increase in mutations was found in DNA from the gastric mucosa of infected $p53^{+/+}$ mice, and also in uninfected $p53^{+/-}$ mice; the mutation frequency in infected $p53^{+/-}$ mice was further increased by approximately threefold. The intensity of inflammation was estimated to be significantly higher in infected $p53^{+/-}$ mice than in infected $p53^{+/+}$ animals, and gastric epithelial proliferation was similarly increased with infection in both latter treatment groups. By contrast, in another study, infection of Big Blue transgenic mice (sex not specified) with the SS1 strain of *H. pylori* for 3.5 mo resulted in no significant increase in gastric mutations over uninfected controls (13).

We used the *gpt* delta mouse to measure the accumulation of gastric mutations associated with *H. pylori* SS1 infection in male and female animals at 6 and 12 MPI. This experimental system comprises λ-EG10–based transgenic C57BL/6 mice harboring tandem arrays of 80 copies of the bacterial *gpt* gene at a single site on chromosome 17. The model was specifically designed to facilitate the in vivo detection of point mutations by 6-thioguanine

Author contributions: A.S., C.W.L., J.G.F., and D.B.S. designed research; A.S., C.W.L., and B.H.R. performed research; K.M. and T.N. contributed new reagents/analytic tools; A.S., B.H.R., G.N.W., J.G.F., and D.B.S. analyzed data; and A.S., G.N.W., and J.G.F. wrote the paper.

The authors declare no conflict of interest.

[1]To whom correspondence should be addressed. E-mail: wogan@mit.edu.

[2]J.G.F. and D.B.S. contributed equally to this work.

This article contains supporting information online at www.pnas.org/lookup/suppl/doi:10.1073/pnas.1009017107/-/DCSupplemental.

MICROBIOLOGY

(6-TG) selection, and deletions up to 10 kb in length by selection based on sensitivity to P2 interference (Spi$^-$) (24). When phage DNA rescued from mouse tissues is introduced into appropriate *Escherichia coli* strains, both point mutations and large deletions can be efficiently detected (24). We also characterized histopathologic changes, expression of inflammatory cytokines, and expression of iNOS in gastric mucosa 6 and 12 mo after initial infection. In addition, we compared responses of male and female mice to assess the influence of sex. We found that *H. pylori* infection induced significant increases in the frequency of point mutations in the gastric mucosa of female, but not male, *gpt* delta mice. The accumulation of point mutations was therefore sex-dependent and was mediated by the duration of infection and the severity of disease.

Results and Discussion

Pathology, Cytokine and iNOS Expression, and Serologic Responses to *H. pylori* Infection and *H. pylori* Levels. Inflammatory histopathologic changes resulting from *H. pylori* infection were evaluated (Fig. S1) and gastric histological activity index (GHAI) scores calculated, with the following results. Scores were significantly increased in infected animals of both sexes at 6 and 12 MPI (female, $P < 0.001$ and $P < 0.01$, respectively; and male, $P < 0.05$ and $P < 0.001$, respectively; Fig. 1). Regarding specific types of lesions represented in the GHAI, infected females experienced higher levels of hyperplasia ($P < 0.05$), epithelial defects ($P < 0.001$), and dysplasia ($P < 0.05$) compared with infected males at 6 MPI, and thus had correspondingly higher ($P < 0.05$) GHAI scores at this time point. At 6 MPI, infected animals of both sexes displayed mild to moderate inflammation, comprised chiefly of submucosal and mucosal infiltrates of mononuclear and granulocytic cells. In addition, in infected males, mucous metaplasia, intestinal metaplasia, oxyntic gland atrophy, and hyalinosis were all significantly elevated compared with controls (all $P < 0.01$; intestinal metaplasia, $P < 0.001$); no significant increases occurred in foveolar hyperplasia, epithelial defects, or dysplasia. In infected females, inflammation ($P < 0.05$), epithelial defects ($P < 0.001$), mucous metaplasia ($P < 0.01$), hyalinosis ($P < 0.001$), as well as premalignant lesions of oxyntic gland atrophy ($P < 0.001$), intestinal metaplasia ($P < 0.05$), and dysplasia ($P < 0.05$) were significantly elevated compared with uninfected controls. At 12 MPI, there were no differences in gastric lesion severity between infected males and females; both groups had similar mucosal changes. Infected male mice at 12 MPI displayed significantly increased epithelial defects but decreased intestinal metaplasia than infected males at 6 MPI ($P < 0.01$ and $P < 0.001$).

H. pylori infection significantly increased transcription profiles at 6 and 12 MPI as follows (details in Fig. S2): *IFNγ* (males, $P < 0.001$; females, $P < 0.01$ at 6 and 12 MPI); *TNF-α* (males, $P < 0.01$ at 6 and 12 MPI; females, $P < 0.01$ and $P < 0.05$); *IL-17* (males, $P < 0.05$ and $P < 0.001$; females, $P < 0.05$ and $P < 0.01$). *iNOS* expression was increased in male and female mice at 6 and 12 MPI (males, $P < 0.05$ and $P < 0.01$; females, $P < 0.01$ and $P < 0.001$) compared with controls at 12 mo. *IL-10* expression was not significantly affected by infection in animals of either sex ($P > 0.05$).

H. pylori infection also resulted in a Th1-predominant IgG2c response in infected mice as previously reported (25, 26) (Fig. 2). *H. pylori*-specific IgG2c levels were higher in infected than in uninfected animals at 6 and 12 MPI ($P < 0.01$ and $P < 0.001$, respectively). At 12 MPI, infected females had significantly higher

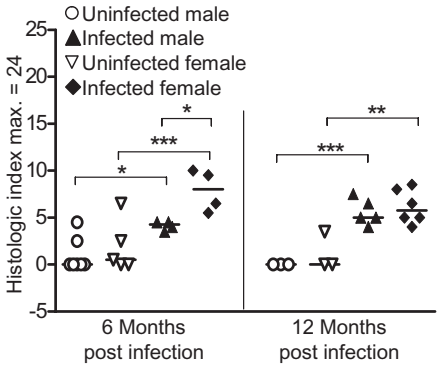

Fig. 1. *H. pylori* infection elicits more gastric pathologic processes in female mice at 6 mo. *H. pylori* infection increased the GHAI in both male and female C57BL/6 mice at 6 and 12 mo. At 6 mo of infection, infected females had significantly more pathologic processes than infected males. Uninfected males (○; 6 MPI, $n = 7$; 12 MPI, $n = 3$), uninfected females (▽; 6 MPI, $n = 5$; 12 MPI, $n = 3$), infected males (▼; 6 MPI, $n = 4$; 12 MPI, $n = 5$) and infected females (◆; 6 MPI, $n = 4$; 12 MPI, $n = 6$). Bar represents the mean. $*P < 0.05$, $**P < 0.01$, and $***P < 0.001$.

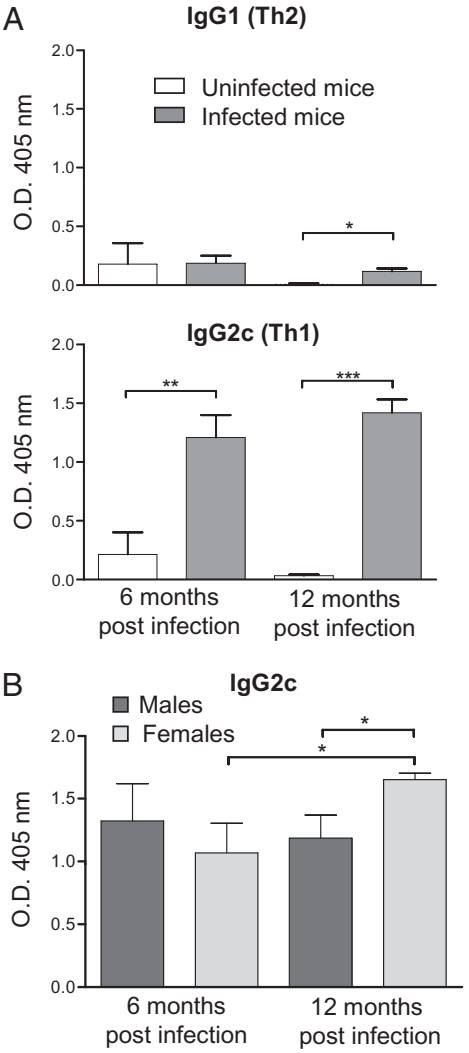

Fig. 2. The effect of *H. pylori* infection on *H. pylori*–specific IgG1 and IgG2c. Serum levels of IgG were measured by ELISA in uninfected and *H. pylori*–infected mice. (*A*) *H. pylori*–infected mice (gray bars; 6 MPI, $n = 9$; 12 MPI, $n = 12$) developed a greater IgG1 response after 12 mo of infection compared with uninfected mice (white bars; 6 MPI, $n = 6$; 12 MPI, $n = 6$; $P < 0.05$). *H. pylori*–infected mice developed a greater IgG2 response after 6 and 12 mo of infection ($P < 0.01$ and $P < 0.001$, respectively). (*B*) At 12 mo, infected female mice (light gray bars; 6 MPI, $n = 4$; 12 MPI, $n = 6$) had substantially increased IgG2c compared with infected males (dark gray bars; 6 MPI, $n = 5$; 12 MPI, $n = 6$) at 12 mo and infected females at 6 mo ($P < 0.05$, both). Data are mean (SE) of mice in different treatment groups. $*P < 0.05$, $**P < 0.01$, and $***P < 0.001$.

IgG2c levels than infected males ($P < 0.05$). Duration of infection also increased IgG2c levels in infected females, with higher levels noted at 12 versus 6 MPI ($P < 0.05$). *H. pylori*-specific IgG1 (Th2) levels were higher in infected than in uninfected animals at 12 MPI ($P < 0.05$). Females had higher Th1/Th2 ratios than males: at 6 MPI, 8.58 vs. 4.01; and at 12 MPI, 12.9 vs. 7.51.

We and others have demonstrated that *H. pylori* levels are inversely correlated with the degree of pathology and the immune response as measured by antibody and cytokine production (25, 27). At 6 MPI, *H. pylori* was detectable by quantitative PCR in all infected males, but not in one female. At 12 MPI, there was a salient difference in levels of *H. pylori* colonization between males and females; *H. pylori* was undetectable in four infected females, but undetectable in only one male (Fig. 3).

Frequency and Nature of Mutations. We determined the frequency of *gpt* point mutations in gastric DNA isolated from infected and uninfected mice by selection of mutants based on 6-TG resistance. Recognizing the possible confounding effect of clonal expansion of sibling mutants (i.e., jackpot mutations), we sequenced the *gpt* genes from all 566 recovered mutants. Any mutation found to duplicate another at the same site within an individual sample was excluded from subsequent frequency calculations. After this adjustment, at 12 MPI the *gpt* mutation frequency in infected females ($7.5 \pm 2.0 \times 10^{-6}$; $P < 0.05$) was significantly (1.6-fold) higher than that in all control animals ($4.7 \pm 1.1 \times 10^{-6}$), whereas the frequency in infected males ($6.3 \pm 5.4 \times 10^{-6}$; $P = 0.49$) was not. At 6 MPI, *gpt* mutation frequency in infected animals of either sex (females, $5.6 \pm 2.0 \times 10^{-6}$, $P = 0.72$; males, $7.2 \pm 2.2 \times 10^{-6}$, $P = 0.57$) was not significantly different from that of controls ($6.2 \pm 3.0 \times 10^{-6}$; Fig. 4).

After sequencing and accounting for clonal expansion, 236 from infected and 156 mutants from uninfected mice were used to identify effects of *H. pylori* infection on types of mutations causing loss of *gpt* function, with the results summarized in Table 1 and Table S1. G:C-to-A:T transitions and G:C-to-T:A transversions were the most prevalent types of mutations in both infected and uninfected animals, representing 33% to 50% and 17% to 31%, respectively, of total mutations in various treatment groups; mutant frequencies varied from 2.1 to 3.0×10^{-6} in these transitions and 0.9–1.8×10^{-6} in the transversions. The 1.6-fold higher total mutations observed in infected females compared with age-matched controls at 12 MPI was attributable mainly to two types of mutations: 3.8 times more A:T-to-G:C transitions ($P < 0.05$) and 2.0 times more G:C-to-T:A transversions ($P < 0.05$). These two mutations are consistent with the expected mutational spectrum induced by RONS (28) and have been found elevated in another animal model of chronic inflammation (13). An increase in G:C-to-T:A transversions was also reported in a previous study documenting *H. pylori*-induced mutations (22).

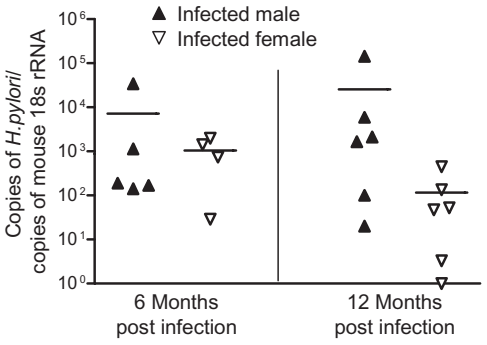

Fig. 3. *H. pylori* levels in the stomach were lower in infected females at 12 MPI. Values represent the number of *H. pylori* organisms per copies of mouse 18s rRNA. At 6 MPI, one infected female mouse was under the threshold of detection (15 copies of *H. pylori*). At 12 MPI, four infected females and one infected male were undetectable. Infected males (▼; 6 MPI, $n = 5$; 12 MPI, $n = 6$) and infected females (▽; 6 MPI, $n = 4$; 12 MPI, $n = 6$). Bar represents the mean.

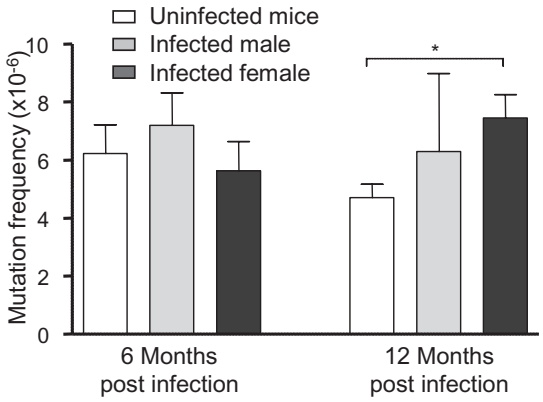

Fig. 4. Twelve-month infection with *H. pylori* increases the frequency of point mutations in female mice. The mutation frequency of point mutations was determined by the *gpt* assay in uninfected mice (white bars; 6 MPI, $n = 13$; 12 MPI, $n = 15$), *H. pylori*-infected males (light gray bars; 6 MPI, $n = 4$; 12 MPI, $n = 5$) and *H. pylori*-infected females (dark gray bars; 6 MPI, $n = 9$; 12 MPI, $n = 11$). Control mice of both sexes were grouped for this analysis. Data are mean (SEM) of mutation frequency of mice in different treatment groups. $*P < 0.05$.

A:T-to-G:C transitions can be formed by deamination of adenine to hypoxanthine or creation of ethenoadenine. Deamination is mediated by N_2O_3, the autoxidation product of NO·, which directly nitrosates primary amines on DNA bases (28, 29). Hypoxanthine resembles guanine and mispairs with cytosine, resulting in the observed mutation. Alternatively, A:T-to-G:C transitions can also be created indirectly by lipid peroxidation by RONS, forming etheno adducts in DNA such as highly mutagenic ethenoadenine (30, 31). G:C-to-T:A transversions have also been associated with increased *iNOS* expression levels, pointing to the involvement of RONS (32). Cells cocultivated with activated macrophages predominantly develop G:C to T:A transversions caused by exposure to NO·, O_2^{-}·, and H_2O_2 (33). G:C-to-T:A transversions are also caused by adducts produced by oxidative stress or lipid peroxidation, such as 8-oxodG, εdC, and M1G (34, 35). The presence of 8-oxodG, a major product of oxidative damage to DNA, results in mispairing of guanine with adenine during replication, thus inducing transversions (36). Although 8-oxodG is believed to be the main cause of this mutation, etheno adducts formed by lipid peroxidation may also play a significant role in mutagenesis observed in vivo (37).

Fig. S3 shows the mutation spectrum detected in the *gpt* gene, of which the following features are noteworthy. In both uninfected and infected mice, hotspots occurred at nucleotides C64, G110, G115, and G418; C64, G110, and G115 are CpG sites and are known hotspots in this assay (38, 39). Hotspots occurring in infected mice were located at A8, G116, and G143; A8 and G116 were found predominantly in infected females at both 6 and 12 mo, whereas G143, located at a CpG site, was a hotspot in infected animals of both sexes. Uninfected mice had hotspots at G406, G416, and A419, one of which (G416) occurred mainly in males. Mutations in infected males were concentrated mainly in hotspots common to both uninfected and infected animals, whereas in infected females there was an increase in mutations throughout the *gpt* gene at non-G:C sites. This result suggests that the chemistry of DNA damage in mice with a stronger host response to infection may have differed from that in mice with mild or minimal gastritis.

Table 1. Twelve months of *H. pylori* infection increases the mutation frequency of A:T-to-G:C transitions and G:C-to-T:A transversions in female mice

Effect	6 mo			12 mo		
	Uninfected all (n = 6)	Infected male (n = 4)	Infected female (n = 8)	Uninfected all (n = 14)	Infected male (n = 5)	Infected female (n = 11)
Transition						
G:C to A:T	3.02 (2.07)	2.41 (2.64)	2.74 (1.07)	2.13 (0.87)	2.66 (1.70)	2.69 (0.97)
A:T to G:C	0.27 (0.61)	0.00	0.16 (0.22)	0.23 (0.19)	0.08 (0.16)	0.88 (0.59)*
Transversion						
G:C to T:A	1.30 (1.34)	1.64 (1.29)	0.89 (0.68)	0.85 (0.62)	1.69 (2.43)	1.75 (0.54)*
G:C to C:G	0.29 (0.66)	0.36 (0.71)	0.40 (0.60)	0.19 (0.27)	0.84 (1.25)	0.09 (0.14)
A:T to T:A	0.34 (0.47)	0.00	0.37 (0.37)	0.31 (0.41)	0.00	0.53 (0.89)
A:T to C:G	0.00	0.36 (0.71)	0.18 (0.22)	0.05 (0.12)	0.00	0.25 (0.46)
Deletion						
1-bp deletion	0.84 (0.94)	2.44 (3.99)	0.66 (0.43)	0.53 (0.35)	0.67 (0.54)	0.88 (0.73)
≥2-bp deletion	0.04 (0.12)	0.00	0.44 (0.57)	0.22 (0.20)	0.18 (0.36)	0.22 (0.34)
Insertion	0.00	0.00	0.08 (0.16)	0.20 (0.23)	0.00	0.11 (0.17)
Complex mutation	0.14 (0.31)	0.00	0.04 (0.08)	0.00	0.18 (0.36)	0.12 (0.29)
Total	6.23 (2.98)	7.20 (2.21)	5.95 (1.54)	4.71 (1.13)	6.29 (5.37)	7.51 (1.91)*

Data are mean (SD) of mutation frequency data from 411 mutants recovered from the *gpt* assay after excluding 155 mutants considered siblings. Control mice of both sexes were grouped for this analysis. The mutation frequency of A:T-to-G:C transitions and G:C-to-T:A transversions was significantly elevated in female mice infected with *H. pylori* for 12 mo.
*$P < 0.05$.

Mutation analysis using the Spi$^-$ assay revealed that the frequency of deletion mutations in *gpt* of gastric tissue DNA was not significantly affected by *H. pylori* infection (Fig. 5). Analyses of 57 samples from 32 mice showed that Spi$^-$ mutant frequencies in infected mice (females at 6 MPI, $4.8 \pm 2.5 \times 10^{-6}$, $P = 0.09$; females at 12 MPI, $5.0 \pm 2.6 \times 10^{-6}$, $P = 0.30$; males at 6 MPI, $6.3 \pm 2.5 \times 10^{-6}$, $P = 0.87$; and males at 12 MPI, $5.2 \pm 1.4 \times 10^{-6}$, $P = 0.17$) were not significantly different from those of age-matched controls at either time point (all mice at 6 MPI, $2.9 \pm 1.3 \times 10^{-6}$; all mice at 12 MPI, $3.6 \pm 1.8 \times 10^{-6}$).

Current models of inflammation-driven carcinogenesis are based on chronic inflammation inducing mutations that lead to cancer (40, 41). Female mice at 6 MPI had more hyperplasia, epithelial defects, and dysplasia than infected males and age-matched controls, but this increase in pathologic findings was not accompanied by increased frequency of mutations. This was detected only in infected female mice at 12 MPI, which had experienced more severe gastritis for a longer period, suggesting that gastritis is necessary but not sufficient to induce mutagenesis. Similarly, duration of infection in itself was insufficient, as mutation frequency was not increased in male mice at 12 MPI. Based on the GHAI, infected male mice had a weaker response at 6 MPI compared with infected females, whereas by 12 MPI, the level of pathologic process was similar in both sexes. These data suggest that the delayed onset of severe gastric lesions in males reduced the duration of their exposure to chronic gastritis, protecting them from mutagenesis, highlighting the importance of severity and duration of the inflammatory response.

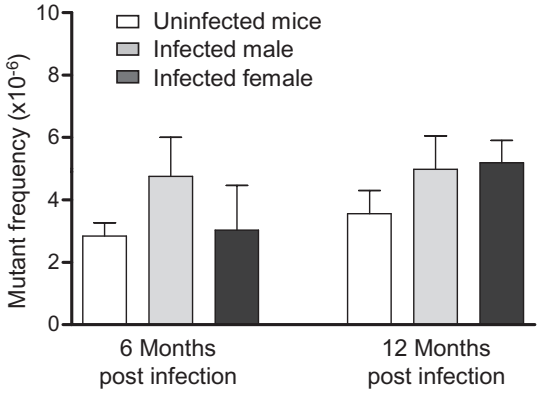

Fig. 5. Mutant frequency of deletions was unchanged by *H. pylori* infection. *H. pylori* infection did not alter the levels of deletions detected by the Spi$^-$ assay in uninfected mice (white bars; 6 MPI, n = 12; 12 MPI, n = 16), *H. pylori*-infected males (light gray bars; 6 MPI, n = 3; 12 MPI, n = 5) and *H. pylori*-infected females (dark gray bars; 6 MPI, n = 9; 12 MPI, n = 12). Control mice of both sexes were grouped for this analysis. Data are mean (SEM) of mutant frequency of mice in different treatment groups.

Our findings agree with current paradigms for the role of inflammation in carcinogenesis (4) and with the more severe pathology induced in female versus male C57BL/6 mice infected with *Helicobacter* spp. (42). Our observations in female *gpt* delta mice are consistent with previously reported data from female C57BL/6 Big Blue mice infected with *H. felis*, which induces more severe gastritis at earlier time points than *H. pylori*, effectively increasing the amount of DNA damage inflicted after infection (23, 43, 44). The higher mutation frequency found at 7 MPI in *H. felis*-infected female C57BL/6 Big Blue mice may be comparable to that occurring at 12 MPI in female *gpt* delta mice infected with *H. pylori*, based on increased inflammation and epithelial proliferation. In contrast, another study of DNA point mutations induced by *H. pylori* in male Big Blue mice reported that, although mutant frequency was increased at 6 MPI, it returned to control levels by 12 MPI (22). The decrease between 6 and 12 MPI was accompanied by loss of *iNOS* expression and reversion of the mutation spectrum to one indistinguishable from that of uninfected mice (22). Two possible explanations for these results are that (*i*) the increase in mutations at 6 MPI may have reflected jackpot mutations, because clonal expansion was not assessed or (*ii*) loss of infection resulted in absence of iNOS expression and reversion of the mutation spectrum. An additional factor pertinent to comparisons of previous mutagenesis studies involving gastric infection by *Helicobacter* spp. is the endogenous *Helicobacter* status of the mouse colony (45). We recently reported that concurrent, subclinical infection in C57BL/6 mice with non-gastric *Helicobacter bilis* significantly reduced *H. pylori*-associated premalignant gastric lesions at 6 and 11 MPI (46). This immunomodulatory effect could affect observed mutagenic responses,

and it is unknown whether Big Blue mice used in previous studies were free of enteric *Helicobacter* spp.

Our observed sex-based effects on mutagenesis induced by *H. pylori* in mice has not been reported previously, but sex bias has been found in other responses to infection. In *H. pylori*–infected Mongolian gerbils, immune responses and cytokine production were reported to be affected by sex (47), and *H. pylori* preferentially induced cancer in male INS-GAS mice (48). Greater female susceptibility to gastric *Helicobacter* infections has been noted previously in WT C57BL/6 mice (42), whereby females infected with *H. felis* experience an earlier onset of gastric inflammation, epithelial hyperplasia, atrophy, and apoptosis (42). Mechanisms responsible for the observed sex-based effects are incompletely understood, but findings to date collectively indicate that sex is an important variable, affecting strength of the host response to *H. pylori* infection, which in turn determines disease outcome.

The typical host response to *Helicobacter* infection is a proinflammatory Th1 response that causes chronic gastritis (49, 50). However, mouse strains such as BALB/c, which mount a strong antiinflammatory Th2 humoral immune response to *H. pylori* infection, develop less severe disease (51). We have previously shown that modulation of the Th1 response by an increased Th2 response reduces pathology associated with concurrent helminth infections (27). In the current study, the immune response of females to *H. pylori* infection was biased toward a greater Th1/Th2 ratio compared with males at both 6 and 12 mo. Higher Th1/Th2 ratios reflect a stronger inflammatory response to *H. pylori* infection. Furthermore, proinflammatory Th17 cells and regulatory T cells have been recently shown to modulate host responses to *H. pylori* (52, 53). *H. pylori*-specific Th17 immunity, mediated by IL-17 (54), increases inflammation unless it is suppressed by regulatory T cells, which are up-regulated by TGF-β and IL-10 (53). Higher levels of inflammation, epithelial defects, and atrophy were indeed observed in infected females at 6 MPI. At 12 MPI, the level of serum IgG2c was significantly elevated in infected females, reflective of increased proinflammatory cytokines in the gastric mucosa, and is consistent with the reduction in *H. pylori* colonization levels. The earlier onset of severe pathologic process caused by the Th1- and Th17-biased response to *H. pylori* was also associated with the increase in point mutations seen at 12 MPI.

In summary, we have shown that chronic *H. pylori* infection can cause premalignant gastric lesions and induce point mutations consistent with inflammatory processes. As our data are derived from analysis of nontranscribed DNA, it serves as an indicator of unbiased mutations reflecting genetic changes during the early stages of tumor initiation in inflamed tissues. At 12 mo, *H. pylori*-infected female C57BL/6 mice accumulate more inflammation-mediated point mutations compared with males as a result of a greater Th1-biased response to infection inducing earlier and more severe pathology. The sex-biased increase in premalignant gastric lesions and induction of mutations highlights the importance of taking into account sex-based effects in future studies of inflammation-driven disease.

Materials and Methods

Bacteria and Animals. *H. pylori* strain SS1 was grown on blood agar or *Brucella* broth with 5% FBS as described in *SI Materials and Methods*. Specific pathogen-free (including *Helicobacter* spp.) male and female C57BL/6 *gpt* delta mice (24) were infected by oral gavage with *H. pylori* SS1 or sham-dosed. At the indicated times, mice were euthanized, gastric tissue collected for histopathology and DNA and RNA extraction, and sera were collected for cytokine and Ig analysis. Gastric lesions were scored for inflammation, epithelial defects, atrophy, hyperplasia, mucous metaplasia, hyalinosis, intestinal metaplasia, and dysplasia using previously published criteria (55). The GHAI is the sum of inflammation, epithelial defects, atrophy, hyperplasia, intestinal metaplasia, and dysplasia scores. A detailed description of the husbandry, treatment, and histopathology is provided in *SI Materials and Methods*.

DNA Isolation and in Vitro Packaging. Genomic DNA was extracted from gastric tissue using RecoverEase DNA Isolation Kit (Stratagene) following the manufacturer's recommendations. λ-EG10 phages were packaged in vitro from genomic DNA using the Transpack Packaging Extract (Stratagene) following the instructions.

***gpt* Assay and Sequencing Analysis.** The 6-TG selection assay was performed as previously described (24, 56). Briefly, phages rescued from murine genomic DNA were transfected into *E. coli* YG6020 expressing Cre recombinase. Infected cells were cultured on plates containing chloramphenicol (Cm) and 6-TG for 3 d until 6-TG–resistant colonies appeared. To confirm the 6-TG–resistant phenotype, colonies were restreaked on plates containing Cm and 6-TG. Confirmed 6-TG–resistant colonies were cultured, and a 739-bp DNA product containing the *gpt* gene was amplified by PCR. DNA sequencing of the *gpt* gene was performed by the Biopolymers Facility at Harvard Medical School (Boston, MA) with AMPure beads (Agencourt) and a 3730xL DNA Analyzer (Applied Biosystems). Sequences were aligned with the *E. coli gpt* gene (GenBank M13422.1) (57) using Geneious (Biomatters). Mutations were classified as transitions, transversions, deletions, insertions, or complex (multiple changes). Duplicate mutations at the same site within an individual tissue were excluded to account for clonal expansion of sibling mutations. More information on primers and methods is provided in *SI Materials and Methods*.

Spi$^-$ Assay. The Spi$^-$ assay was performed as described in *SI Materials and Methods*. Briefly, phages rescued from murine genomic DNA were transfected into *E. coli* strains with or without P2 lysogen. Infected cells were cultured overnight on λ-trypticase agar plates to allow plaque formation. The inactivation of *red* and *gam* genes was confirmed by respotting plaques on another *E. coli* strain with P2 lysogen (24).

mRNA Expression. RNA was extracted from gastric tissue and reverse-transcribed to cDNA. Quantitative real-time PCR was performed using TaqMan Gene Expression Assays (Applied Biosystems). TaqMan primers and analysis methods are described in *SI Materials and Methods*.

***H. pylori* Detection.** *H. pylori* levels in the gastric mucosa were quantified by real-time quantitative PCR assay of gastric DNA as described in *SI Materials and Methods*. A threshold of 15 copies of the *H. pylori* genome was set as the lower limit for a positive sample.

Serum IgG Isotype Measurement. Sera were analyzed for *H. pylori*-specific IgG2c and IgG1 by ELISA. Additional information on the measurements is provided in *SI Materials and Methods*.

Statistical Analysis. Two-way ANOVA followed by Bonferroni posttests were used to analyze GHAI and mRNA expression values. Student two-tailed *t* tests were used to analyze mutant and mutation frequency data and serum IgG isotypes. Poisson distribution analysis was used to determine hotspots at a 99% confidence level (58). For some analyses, age-matched controls of both sexes were grouped when no statistical differences were detected between sexes. Analyses were done with GraphPad Prism, version 4.0, or Microsoft Excel 2002. $P < 0.05$ was considered significant.

ACKNOWLEDGMENTS. We thank Sureshkumar Muthupalani for help with the histological images and Laura J. Trudel for assistance with the manuscript and figures. This study is dedicated in loving memory of David Schauer, a mentor and a friend, for his contribution in the design and analysis of this work. This work was supported by National Institutes of Health Grants R01-AI037750 and P01-CA026731 and Massachusetts Institute of Technology Center for Environmental Health Sciences Program Project Grant P30-ES02109.

1. Fox JG, Wang TC (2007) Inflammation, atrophy, and gastric cancer. *J Clin Invest* 117: 60–69.
2. Suerbaum S, Michetti P (2002) Helicobacter pylori infection. *N Engl J Med* 347:1175–1186.
3. International Agency for Research on Cancer (1994) Schistosomes, liver flukes and Helicobacter pylori. IARC Working Group on the Evaluation of Carcinogenic Risks to Humans. Lyon, 7-14 June 1994. *IARC Monogr Eval Carcinog Risks Hum* 61:1–241.
4. Coussens LM, Werb Z (2002) Inflammation and cancer. *Nature* 420:860–867.
5. Obst B, Wagner S, Sewing KF, Beil W (2000) Helicobacter pylori causes DNA damage in gastric epithelial cells. *Carcinogenesis* 21:1111–1115.
6. Xu H, et al. (2004) Spermine oxidation induced by Helicobacter pylori results in apoptosis and DNA damage: Implications for gastric carcinogenesis. *Cancer Res* 64: 8521–8525.

7. Davies GR, et al. (1994) Relationship between infective load of Helicobacter pylori and reactive oxygen metabolite production in antral mucosa. *Scand J Gastroenterol* 29: 419–424.
8. Davies GR, et al. (1994) Helicobacter pylori stimulates antral mucosal reactive oxygen metabolite production in vivo. *Gut* 35:179–185.
9. Mannick EE, et al. (1996) Inducible nitric oxide synthase, nitrotyrosine, and apoptosis in Helicobacter pylori gastritis: Effect of antibiotics and antioxidants. *Cancer Res* 56: 3238–3243.
10. Meira LB, et al. (2008) DNA damage induced by chronic inflammation contributes to colon carcinogenesis in mice. *J Clin Invest* 118:2516–2525.
11. Nair J, et al. (2006) Increased etheno-DNA adducts in affected tissues of patients suffering from Crohn's disease, ulcerative colitis, and chronic pancreatitis. *Antioxid Redox Signal* 8:1003–1010.
12. Zhuang JC, Lin C, Lin D, Wogan GN (1998) Mutagenesis associated with nitric oxide production in macrophages. *Proc Natl Acad Sci USA* 95:8286–8291.
13. Sato Y, et al. (2006) IL-10 deficiency leads to somatic mutations in a model of IBD. *Carcinogenesis* 27:1068–1073.
14. Bartsch H, Nair J (2004) Oxidative stress and lipid peroxidation-derived DNA-lesions in inflammation driven carcinogenesis. *Cancer Detect Prev* 28:385–391.
15. Nair U, Bartsch H, Nair J (2007) Lipid peroxidation-induced DNA damage in cancer-prone inflammatory diseases: a review of published adduct types and levels in humans. *Free Radic Biol Med* 43:1109–1120.
16. Kang JM, Iovine NM, Blaser MJ (2006) A paradigm for direct stress-induced mutation in prokaryotes. *FASEB J* 20:2476–2485.
17. Crabtree JE, Ferrero RL, Kusters JG (2002) The mouse colonizing Helicobacter pylori strain SS1 may lack a functional cag pathogenicity island. *Helicobacter* 7:139–140, author reply 140–141.
18. Lee A, Mitchell H, O'Rourke J (2002) The mouse colonizing Helicobacter pylori strain SS1 may lack a functional cag pathogenicity island: Response. *Helicobacter* 7:140–141.
19. Miyazawa M, et al. (2003) Suppressed apoptosis in the inflamed gastric mucosa of *Helicobacter pylori*-colonized iNOS-knockout mice. *Free Radic Biol Med* 34:1621–1630.
20. Jang J, et al. (2003) Malgun (clear) cell change in *Helicobacter pylori* gastritis reflects epithelial genomic damage and repair. *Am J Pathol* 162:1203–1211.
21. Lee H, et al. (2000) "Malgun" (clear) cell change of gastric epithelium in chronic *Helicobacter pylori* gastritis. *Pathol Res Pract* 196:541–551.
22. Touati E, et al. (2003) Chronic Helicobacter pylori infections induce gastric mutations in mice. *Gastroenterology* 124:1408–1419.
23. Jenks PJ, Jeremy AH, Robinson PA, Walker MM, Crabtree JE (2003) Long-term infection with Helicobacter felis and inactivation of the tumour suppressor gene p53 cumulatively enhance the gastric mutation frequency in Big Blue transgenic mice. *J Pathol* 201:596–602.
24. Nohmi T, et al. (1996) A new transgenic mouse mutagenesis test system using Spi- and 6-thioguanine selections. *Environ Mol Mutagen* 28:465–470.
25. Ihrig M, Whary MT, Dangler CA, Fox JG (2005) Gastric helicobacter infection induces a Th2 phenotype but does not elevate serum cholesterol in mice lacking inducible nitric oxide synthase. *Infect Immun* 73:1664–1670.
26. Lee CW, et al. (2008) Helicobacter pylori eradication prevents progression of gastric cancer in hypergastrinemic INS-GAS mice. *Cancer Res* 68:3540–3548.
27. Fox JG, et al. (2000) Concurrent enteric helminth infection modulates inflammation and gastric immune responses and reduces helicobacter-induced gastric atrophy. *Nat Med* 6:536–542.
28. De Bont R, van Larebeke N (2004) Endogenous DNA damage in humans: A review of quantitative data. *Mutagenesis* 19:169–185.
29. Burney S, Caulfield JL, Niles JC, Wishnok JS, Tannenbaum SR (1999) The chemistry of DNA damage from nitric oxide and peroxynitrite. *Mutat Res* 424:37–49.
30. Kadlubar FF, et al. (1998) Comparison of DNA adduct levels associated with oxidative stress in human pancreas. *Mutat Res* 405:125–133.
31. Pandya GA, Moriya M (1996) 1, N6-ethenodeoxyadenosine, a DNA adduct highly mutagenic in mammalian cells. *Biochemistry* 35:11487–11492.
32. Ambs S, et al. (1999) Relationship between p53 mutations and inducible nitric oxide synthase expression in human colorectal cancer. *J Natl Cancer Inst* 91:86–88.
33. Kim MY, Wogan GN (2006) Mutagenesis of the supF gene of pSP189 replicating in AD293 cells cocultivated with activated macrophages: roles of nitric oxide and reactive oxygen species. *Chem Res Toxicol* 19:1483–1491.
34. Dedon PC, Plastaras JP, Rouzer CA, Marnett LJ (1998) Indirect mutagenesis by oxidative DNA damage: formation of the pyrimidopurinone adduct of deoxyguanosine by base propenal. *Proc Natl Acad Sci USA* 95:11113–11116.
35. Jackson AL, Loeb LA (2001) The contribution of endogenous sources of DNA damage to the multiple mutations in cancer. *Mutat Res* 477:7–21.
36. Wood ML, Esteve A, Morningstar ML, Kuziemko GM, Essigmann JM (1992) Genetic effects of oxidative DNA damage: comparative mutagenesis of 7,8-dihydro-8-oxoguanine and 7,8-dihydro-8-oxoadenine in Escherichia coli. *Nucleic Acids Res* 20: 6023–6032.
37. Pang B, et al. (2007) Lipid peroxidation dominates the chemistry of DNA adduct formation in a mouse model of inflammation. *Carcinogenesis* 28:1807–1813.
38. Masumura K, et al. (2003) Low dose genotoxicity of 2-amino-3,8-dimethylimidazo[4,5-f]quinoxaline (MeIQx) in gpt delta transgenic mice. *Mutat Res* 541:91–102.
39. Masumura K, et al. (2000) Characterization of mutations induced by 2-amino-1-methyl-6-phenylimidazo[4,5-b]pyridine in the colon of gpt delta transgenic mouse: novel G:C deletions beside runs of identical bases. *Carcinogenesis* 21:2049–2056.
40. Balkwill F, Coussens LM (2004) Cancer: An inflammatory link. *Nature* 431:405–406.
41. Clevers H (2004) At the crossroads of inflammation and cancer. *Cell* 118:671–674.
42. Court M, Robinson PA, Dixon MF, Jeremy AH, Crabtree JE (2003) The effect of gender on Helicobacter felis-mediated gastritis, epithelial cell proliferation, and apoptosis in the mouse model. *J Pathol* 201:303–311.
43. Fox JG, et al. (2002) Germ-line p53-targeted disruption inhibits helicobacter-induced premalignant lesions and invasive gastric carcinoma through down-regulation of Th1 proinflammatory responses. *Cancer Res* 62:696–702.
44. Lee A, Fox JG, Otto G, Murphy J (1990) A small animal model of human Helicobacter pylori active chronic gastritis. *Gastroenterology* 99:1315–1323.
45. Taylor NS, et al. (1995) Long-term colonization with single and multiple strains of Helicobacter pylori assessed by DNA fingerprinting. *J Clin Microbiol* 33:918–923.
46. Lemke LB, et al. (2009) Concurrent Helicobacter bilis infection in C57BL/6 mice attenuates proinflammatory *H. pylori*-induced gastric pathology. *Infect Immun* 77: 2147–2158.
47. Crabtree JE, et al. (2004) Gastric mucosal cytokine and epithelial cell responses to Helicobacter pylori infection in Mongolian gerbils. *J Pathol* 202:197–207.
48. Fox JG, et al. (2003) Host and microbial constituents influence Helicobacter pylori-induced cancer in a murine model of hypergastrinemia. *Gastroenterology* 124:1879–1890.
49. Bamford KB, et al. (1998) Lymphocytes in the human gastric mucosa during Helicobacter pylori have a T helper cell 1 phenotype. *Gastroenterology* 114:482–492.
50. Mohammadi M, Czinn S, Redline R, Nedrud J (1996) Helicobacter-specific cell-mediated immune responses display a predominant Th1 phenotype and promote a delayed-type hypersensitivity response in the stomachs of mice. *J Immunol* 156: 4729–4738.
51. Sakagami T, et al. (1996) Atrophic gastric changes in both Helicobacter felis and Helicobacter pylori infected mice are host dependent and separate from antral gastritis. *Gut* 39:639–648.
52. Lee CW, et al. (2007) Wild-type and interleukin-10-deficient regulatory T cells reduce effector T-cell-mediated gastroduodenitis in Rag2-/- mice, but only wild-type regulatory T cells suppress Helicobacter pylori gastritis. *Infect Immun* 75:2699–2707.
53. Kao JY, et al. (2010) Helicobacter pylori immune escape is mediated by dendritic cell-induced Treg skewing and Th17 suppression in mice. *Gastroenterology* 138:1046–1054.
54. Xu S, Cao X (2010) Interleukin-17 and its expanding biological functions. *Cell Mol Immunol* 7:164–174.
55. Rogers AB, et al. (2005) Helicobacter pylori but not high salt induces gastric intraepithelial neoplasia in B6129 mice. *Cancer Res* 65:10709–10715.
56. Masumura K, et al. (1999) Spectra of gpt mutations in ethylnitrosourea-treated and untreated transgenic mice. *Environ Mol Mutagen* 34:1–8.
57. Nüesch J, Schümperli D (1984) Structural and functional organization of the gpt gene region of Escherichia coli. *Gene* 32:243–249.
58. Kim MY, Dong M, Dedon PC, Wogan GN (2005) Effects of peroxynitrite dose and dose rate on DNA damage and mutation in the supF shuttle vector. *Chem Res Toxicol* 18: 76–86.